

**PSFC/JA-03-25**

**Control of Internal Transport Barriers on Alcator C-Mod**

C.L. Fiore, P.T. Bonoli, D.R. Ernst, A.E. Hubbard, M.J.  
Greenwald, A. Lynn, E.S. Marmor, P. Phillips,<sup>a</sup> M.H. Redi,<sup>b</sup> J.E.  
Rice, S.M. Wolfe, S.J. Wukitch, K. Zhurovich

November 4, 2003

Plasma Science and Fusion Center  
Massachusetts Institute of Technology  
Cambridge, MA 02139 USA

<sup>a</sup> present address: Fusion Research Center, University of Texas at Austin, Austin, TX  
<sup>b</sup> present address: Princeton Plasma Physics Laboratory, Princeton, NJ

This work was supported by the U.S. Department of Energy, Cooperative Grant No. DE-FC02-99ER54512. Reproduction, translation, publication, use and disposal, in whole or in part, by or for the United States government is permitted.

Submitted for publication to *Physics of Plasmas*.

# Control of Internal Transport Barriers on Alcator C-Mod

C.L. Fiore, P. T. Bonoli, D. R. Ernst, A. E. Hubbard, M. J. Greenwald, A. Lynn,<sup>a</sup> E. S. Marmor, P. Phillips,<sup>a</sup> M. H. Redi,<sup>b</sup> J. E. Rice, S. M. Wolfe, S. J. Wukitch, K. Zhurovich  
Plasma Science and Fusion Center, Massachusetts Institute of Technology, Cambridge, MA 02139; <sup>a</sup> Fusion Research Center, University of Texas at Austin, Austin, TX; <sup>b</sup>Princeton Plasma Physics Laboratory, Princeton, NJ

## Abstract

Recent studies of internal transport and double transport barrier regimes in Alcator C-Mod [I. H. Hutchinson, *et al.*, Phys. Plasmas **1**, 1511 (1994)] have explored the limits for forming, maintaining, and controlling these plasmas. C-Mod provides a unique platform for studying such discharges: the ions and electrons are tightly coupled by collisions and the plasma has no internal particle or momentum sources. The double-barrier mode comprised of an edge barrier with an internal transport barrier (ITB) can be induced at will using off-axis ion cyclotron range of frequency (ICRF) injection on either the low or high field side of the plasma with either of the available ICRF frequencies (70 or 80 MHz). When enhanced  $D_\alpha$  high confinement mode (EDA H-mode) is accessed in Ohmic plasmas, the double barrier ITB forms spontaneously if the H-mode is sustained for  $\sim 2$  energy confinement times. The ITBs formed in both Ohmic and ICRF heated plasmas are quite similar regardless of the trigger method. They are characterized by strong central peaking of the electron density, and reduction of the core particle and energy

transport. Control of impurity influx and heating of the core plasma in the presence of the ITB have been achieved with the addition of central ICRF power in both Ohmic H-mode and ICRF induced ITBs. The radial location of the particle transport is dependent on the toroidal magnetic field but not on the location of the ICRF resonance. A narrow region of decreased electron thermal transport, as determined by sawtooth heat pulse analysis, is found in these plasmas as well. Transport analysis indicates that reduction of the particle diffusivity in the barrier region allows the neoclassical pinch to drive the density and impurity accumulation in the plasma center. Examination of the gyrokinetic stability at the trigger time for the ITB suggests that the density and temperature profiles are inherently stable to ion temperature gradient (ITG) and trapped electron (TEM) modes in the core inside of the ITB location.

Catherine L. Fiore

MIT Room NW21-203

77 Mass. Ave.

Cambridge, MA 02139

USA

Fiore@psfc.mit.edu

## I. Introduction

Transport barriers, both edge and internal, have been widely reported in most major magnetic plasma experiments worldwide. Wolf<sup>1</sup> has provided a comprehensive review of the experimental results and current understanding of these phenomena. Most experiments have achieved internal transport barriers (ITBs) by adding auxiliary heating<sup>2,3,4,5,6</sup> beyond some threshold value resulting in distinct changes in the heat, momentum, or particle transport from one region of the plasma to another. It has also been demonstrated that reversal of magnetic shear by use of current modification by lower hybrid current drive<sup>7</sup> or electron cyclotron current drive<sup>8</sup> encourages ITB development. These are thought to occur when the effects of pressure profile gradient driven instabilities are reduced by the introduction of rotational shear into the unstable region or by providing a region of reversed magnetic shear<sup>9</sup>.

Internal transport barriers are achieved routinely under specific conditions in the Alcator C-Mod plasmas.<sup>10,11,12,13</sup> While several different criteria are often used to define an ITB, the most general definition maintains that an ITB exists in the plasma when there is a clear change in the plasma transport at an internal boundary in some quantity such as energy, particles, or momentum<sup>14</sup>. Steady state ITBs (lasting at least 10 energy confinement times) arise during EDA H-mode plasmas when either the H-mode is produced in an Ohmic plasma or when ICRF heating is applied well off axis, typically with the resonance location being at or greater than  $r/a=0.5$  on either the low or high field side of the plasma. The H-mode edge transport barrier is maintained throughout so that double transport barriers exist for these ITB plasmas. The presence of the barrier is most obvious from the electron density profile where a sharp break in the slope of the profile is seen in the vicinity of the half radius of the plasma. While a similar change in the slope is not observed in the electron temperature profile (the ion temperature

profile is not measured routinely) , transport calculations indicate that the effective heat flux from the core of the plasma is reduced significantly, reaching neoclassical levels, once the barrier in the density profile has been established. In addition, a narrow region of decreased electron heat transport as determined from analysis of the heat pulse following a sawtooth crash is observed at or near the location of the break in the density profile<sup>12</sup>. ITBs in Alcator C-Mod are often accompanied by a reduction and sometimes reversal of the central rotation velocity determined by Doppler shifts of the argon impurity line radiation<sup>10,13,15</sup>. It should be noted that most of the discharges discussed here are sawtoothing throughout the ITB presence indicating that the q profile increases monotonically and that the magnetic shear is positive in the ITB region.

Alcator C-Mod<sup>16</sup> is a compact (major radius=0.67 m, minor radius=0.22 m), high field tokamak (toroidal field up to 8T, plasma current up to 1.6 MA) which is routinely operated at very high density ( $0.8 \times 10^{20}$  to  $1 \times 10^{21}/\text{m}^3$ ). At this time, the only source of auxiliary heating is from ICRF, with up to 6 MW available power. Typical operation uses ICRF hydrogen minority heating (deuterium majority) with balanced phasing which provides no particle or momentum sources to the plasma. The experiments discussed here used the ICRF configured with two frequencies: 80 MHz divided between two two-strap antennas and 70 MHz using one four-strap antenna. Thus the Alcator C-Mod plasma provides an ideal proxy for reactor like conditions:  $T_i = T_e$  in thermal equilibration, at high magnetic field and density, with zero applied torque. Results from recent experiments in producing the ITB and controlling its location and the particle accumulation will be described here.

## **II. Production of ITBs in Alcator C-Mod**

ITBs which last ten or more confinement times arise in Alcator C-Mod when the plasma conditions are conducive to spontaneous peaking of the central density. This occurs commonly in H-mode plasmas which exhibit enhanced  $D_\alpha$  (EDA) emission from the edge which have been formed when ICRF power is injected into the plasma with the resonance location placed off-axis, on either the low or high field side of the plasma. The best results are obtained with the resonance position located at or slightly greater than  $r/a=0.5$ . An example of this is shown in Fig. 1a, where the density,  $n_e$ , is derived from the profiles of the visible bremsstrahlung radiation,  $V_b = n_e^2 Z_{\text{eff}}$  where  $Z_{\text{eff}}$  is the average charge state of the plasma.  $Z_{\text{eff}}$  is between 1 and 2 for most Alcator C-Mod plasmas and has a flat radial profile for most operation. The peaking of the density as a function of time is shown in Fig. 1b.  $Z_{\text{eff}}$  becomes somewhat centrally peaked when a strong ITB is present as can be seen from comparison with the density profile obtained from Thomson scattering shown in Fig 1.c. Comparison of the peak values from the two plots at  $t=1.25$  indicates the central  $Z_{\text{eff}}$  reaches a value of 1.65 in this case. Once the EDA H-mode is established, the density inside of the position of the barrier foot ( $0.2 < r/a < 0.6$ ) begins to rise and the characteristic ITB profile is soon apparent. After the ITB has been established, a small amount of central ICRF power is added and is used to clamp successfully further particle and impurity accumulation in the center.

Similar behavior arises when an EDA H-mode is established in a purely Ohmic plasma. In Fig. 2, once again the central density begins to rise steadily shortly after the onset of H-mode, and like the previous case, the particle accumulation can be clamped with addition of a small amount of central ICRF power.

Analysis of the transport parameters using the TRANSP code<sup>17</sup> for these plasmas shows that the central heat conductivity,  $\chi_{\text{eff}}$ , becomes very low after the onset of the ITB, reaching the

neoclassical value at and to the inside of the transport barrier location. ( $\chi_{\text{eff}}$  is used here because  $T_e \cong T_i$  in these plasmas and it is difficult to separate the electron and ion heat conductivities.) This is true for both the spontaneous ITBs in Ohmic EDA H-mode plasmas (Fig. 3.a) as and the off-axis ICRF generated ITBs (Fig 3.b). The bootstrap current, shown in Fig. 4.a, inside of the barrier region increases by as much as 10 times as the ITB develops in these plasma, achieving a local value of 10-12% of the Ohmically induced current. Again, the bootstrap current achieved in these ITB plasmas is the same for both Ohmic EDA H-mode plasma (Fig. 4.b) and off-axis ICRF generated ITBs.

The calculated (TRANSP with the TORIC<sup>16</sup> rf code) net power density distribution (input power minus radiated power) for these ITB plasmas is shown in Fig. 5. As expected, when off-axis ICRF heating is applied at  $r/a=0.5$ , the power density profile is markedly hollow. It is also the case that the power density profile is hollow and peaked off-axis during Ohmic EDA H-mode ITBs as well. Because the plasma continues to exhibit sawtooth activity throughout the ITB phase, the safety factor  $q$  is maintained near to and slightly below 1 in the plasma core and the plasma current is flattened at the center while the toroidal voltage profile increases with radius. The resulting power density profiles and  $\chi_{\text{eff}}$  in both cases are quite similar. It is also shown in this figure that once central ICRF power is added in both cases, the power density becomes peaked on axis.

One result of reducing the central power in the plasma is that the sawtooth oscillations have smaller amplitude than in cases with peaked power density on axis. The electron temperatures at several core radii for two discharges are compared in Fig. 6. These shots were taken on the same day with the same magnetic field, plasma current, target density, and total rf power. In the first case, the rf power was at 70 MHz so that the rf resonance was off axis on the

high field side, and an ITB developed. For the second shot, the rf power was at 80 MHz which was resonant at the plasma center, and no ITB formed. These smaller sawteeth are less perturbative to the temperature and density profiles, and in particular to the gradients of these profiles. The electron temperature in particular becomes quite peaked inside the inversion radius as the sawtooth progresses when the plasma is heated on axis, but has no significant change in gradient when the power is applied off-axis. This can be seen clearly when the profiles are compared in Fig. 7 for the two discharges described in Fig. 6. The steepening of the temperature profile with the application of central power likely contributes to the development of unstable pressure gradient driven modes in the plasma.

Both linear and non-linear modeling of the gyrokinetic stability of the off-axis heated ITB plasma using the GS2 code<sup>19</sup> has demonstrated that there are no strongly growing gradient driven, long wavelength, micro-instabilities at the location of the ITB at the time of the ITB onset,<sup>20</sup> when the density profile is still relatively flat and characteristic of H-mode. Even in the central core of the plasma turbulence is predicted to be minimal. Essentially, the profile conditions are such that the plasma is stable to long wavelength drift modes: ion temperature gradient modes as well as trapped electron mode instabilities at the barrier location. Redi *et al.*<sup>20</sup> have shown in their analysis of the sensitivity of the stability of the barrier and core regions of the plasma at the time of ITB onset that the growth rates are significantly more affected by steepening of the temperature profile than by flattening of the density profile. In short, the plasma density profile is far from marginal stability while the temperature profile is quite close to its critical gradient.

### **III. Control of the ITB Location**



An essential element of controlling the location of the ITB is to determine when an ITB has formed and where it is located in the plasma. The profiles of density and/or temperature typically show a break in the slope where it can be inferred that the transport is different on either side of this position or ITB “foot”. Quantifying this information in a consistent manner that can be applied to a large data set is challenging, particularly for plasmas profiles where the change of slope is more gradual. For the JET tokamak, Tresset<sup>21</sup> et al demonstrated that the dimensionless quantity  $\rho_T^*$ , defined to be the ratio of the Larmor radius at the ion sound speed ( $\rho_s$ ) to the temperature gradient scale length  $L_T$  ( $1/L_T = 1/T \, dT/dr$ ) exceeds a critical value of 0.014 when an ITB is present. Other experiments such as the FTU tokamak at Frascati<sup>22</sup> have found that the ITBs are well characterized by this parameter as well, also at a critical value of 0.014. This parameter is in effect a proxy for the ratio of the E x B shearing rate to the maximum linear growth rate of the pressure gradient driven modes.

On Alcator C-Mod, there is no strong obvious change in the slope of the electron temperature profile at the ITB location. (Ion temperature profile data are not available.) The ITB must be located from the density profile, which can be done by fitting a function (in this case the sum of a Gaussian and parabolic form) to the data to obtain smooth profiles and by then taking the 2<sup>nd</sup> derivative of the resulting profile to determine the inflection point. It was also suggested by Rice<sup>15</sup> that for an experiment which has an ITB which is most visible in the density profile, use of a similar dimensionless parameter to the JET criterion  $\rho_T^* > 0.014$  based on the pressure profile rather than the temperature profile would be useful for determining the presence of an ITB in the plasma. Although the ITB in JET is seen primarily in the temperature profile while it is seen in the density profile on Alcator C-Mod, in fact the pressure profiles of the two experiments in the ITB phase are quite similar in both shape and magnitude.

The quantity  $\rho^*_P$ , defined as  $\rho_s/L_P$  where  $1/L_P=1/P \, dP/dr$ , is plotted as a function of radius in Fig.8 during the ITB phase of an Alcator C-Mod off-axis heated ITB plasma. It can be seen that although neither  $\rho^*_T$  nor  $\rho^*_N = \rho_s/L_N$  exceeds the JET value of 0.014,  $\rho^*_P$ , which is the sum of the two, is higher than 0.014 in part of the core region of the plasma. Comparison of the location where  $\rho^*_P$  begins to exceed 0.014 to the position chosen for the ITB foot by the method of taking the derivative of a functional fit to the data indicates good agreement between the two methods. It should also be noted that at the point where  $\rho^*_T=\rho^*_N$  the ratio of the density gradient scale length to the temperature gradient scale length ( $\eta_i$ ) is equal to 1 and that this location also tends to be near the barrier location.

The location of the ITB foot is plotted as a function of the toroidal field in Fig. 9a. It can be seen that the ITB narrows with increasing magnetic field. It is significant that the location does not appear to depend on the position of the ICRF resonance, which was held nominally at  $r/a = 0.5$ . The 80 MHz ICRF resonance is at  $r/a=0.5$  on the high field side of the plasma at 4.5 T, while at 5.5 T the 70 MHz ICRF resonance is at  $r/a=0.5$  on the low field side. The 80 MHz resonance was placed at  $r/a =0.5$  on the low field side of the plasma at the highest field used here, 6.3T. At the higher fields, the foot position is well separated from the ICRF resonance location.

Regression analysis of the dependence of the ITB foot location on plasma current  $I_p$ , inverse toroidal field  $1/B_t$  and the ratio  $I_p/B_t$  gives correlation values of 0.18, 0.57 and 0.68 respectively. The somewhat stronger correlation with the ratio of plasma current to the magnetic field (Fig. 9b) suggests that the ITB location maybe influenced by the value of  $q_{95}$  or the  $q$  profile. The foot position itself lies in a narrow band of local  $q$  values (determined by fitting the magnetic data) between 1.1 and 1.35.

#### IV. Control of the Core Transport and Particle Accumulation

Typically, during the ITB phase of an Alcator C-Mod discharge, the particle and impurity influx is continuous until either the current is brought down to end the discharge or the radiation level increases to the point where the plasma undergoes a back transition to L-mode. It was demonstrated previously that this continued particle accumulation in the plasma core could be halted by the application of a small amount of central ICRF heating while preserving the ITB profile.<sup>12,13</sup>

The effect of incrementally adding central ICRF power to an established ITB plasma was explored using Ohmic EDA H-mode plasmas. A reproducible target ITB was formed after setting up an EDA H-mode in an Ohmic plasma and then increasing amounts of ICRF power were added over a series of discharges. The results are shown in Fig.10. The lowest amount of power, 0.2 MW, had no effect on the ITB either to impede the particle influx or to modify the profiles. Increasing the power beyond that halted further rise in the central density, with higher powers clamping the central density at progressively lower values. This demonstrated that a desired level of density could be effectively selected by choosing a value for the incremental central ICRF power. The ITB profile was not disturbed by this additional power, and an added benefit was seen in a modest increase in the central ion temperature.

Further addition of central ICRF at or above 1 MW leads to the destruction of the ITB profile. As can be seen in Fig. 11, which shows a series of off-axis ICRF generated ITB plasmas, the central density peaking is clamped by adding up to 0.6 MW of central ICRF. Increasing the central power beyond this level causes the peaking to be lost, and the higher the power the more rapid the degradation. It is also evident from the surface and contour plot of  $\rho_p^*$  shown in Fig. 12 that sawtooth oscillations are altering the pressure gradients in the plasma. The

presence of the ITB is noted by the presence of the black contour which marks the boundary for  $\rho_p^*$  to exceed 0.014. The sawteeth are seen in the peaking and flattening of  $\rho_p^*$  after central ICRF is applied. The value of  $\rho_p^*$  is diminishing on subsequent sawteeth until the ITB is gone with the  $\rho_p^* = 0.014$  level disappearing from the core.

Ernst *et al.*<sup>23</sup> have used gyrokinetic stability code calculations (GS2) to investigate the mechanism for the additional central power to clamp the further density rise. They have identified increased instability of the trapped electron mode (TEM) driven by steepening temperature gradients as the likely mechanism.

## V. Discussion

ITBs can be readily produced in EDA H-mode plasmas on Alcator C-Mod by keeping the input power density peaked off-axis. This can be accomplished by using off-axis ICRF power injection, and it occurs naturally in Ohmic EDA plasmas. Gyrokinetic stability modeling has demonstrated that the pressure profile on Alcator C-Mod is stable to gradient driven long wavelength modes at the time of the ITB onset, and that the electron temperature profile is very close to marginal stability. Coupled with the observation that the application of central heating power enhances the amplitude of sawtooth oscillations, this suggests that the steeper temperature gradients seen in strongly sawtoothing plasmas may prevent the formation of ITBs when power is applied centrally. The steeper temperature profiles are also likely to play a role in controlling the central density rise with small amounts of ICRF power as well.

The position of the ITB foot can be moved outward by lowering the applied toroidal magnetic field. When the ICRF resonance is at  $r/a = 0.5$  on the low field side of the plasma (i. e. at higher toroidal magnetic field), the foot position is significantly to the inside of the resonance layer. This position can be determined from the gradient of the density profile, which happens to

correspond to the same location determined from calculating the dimensionless parameter  $\rho_p^*$  and comparing it to the JET ITB criterion  $\rho_p^* > 0.014$ . This movement of the ITB location could well be determined by  $q$  rather than  $B_t$  directly, and warrants more careful study. The foot location corresponds to a narrow range of local  $q$  values between 1.1 and 1.35. The presence of several low order rational  $q$  surfaces in this region may echo results found on several other experiments connecting ITB formation to the presence of specific low order rational  $q$  surfaces in the plasma, although it lies well inside of the  $q=2$  and  $q=3/2$  surfaces which have been important in other devices.<sup>24</sup>

The rise of the central density and impurity accumulation in the ITB phase of the discharge are clamped by the addition of small amounts of central ICRF power, keeping the central  $Z_{\text{eff}}$  level typically below 2. To date, however, exceeding a certain threshold power destroys the ITB profile. It is not clear that this threshold poses an absolute limit, however, and experiments are planned to test variations in the applied power profiles accordingly.

Future experiments are planned to study ITBs by controlling the plasma current and  $q$ -profile through the use of lower hybrid current drive. In addition, it will be attempted to increase the size of the ITB by operating at even lower applied toroidal field and using a lower ICRF frequency, 50 MHz, for off-axis ICRF heating. Gyrokinetic stability modeling of the experimental results will continue in the hopes of yielding further understanding of the physical mechanisms underlying these behaviors.

## **VI. Acknowledgements**

This work is support by D.o. E. Coop. Agreement DE-FC02-99ER54512. The authors would like to thank Jerry Hughes and Dimitri Mossessian for Thomson scattering density

profiles, Y. Lin for ICRF operation, and Jim Irby and the Alcator C-Mod Operations Group for their support of this work.

## VII. References

- <sup>1</sup>R. C. Wolf, *Plasma Physics and Controlled Fusion* **45**, R1 (2003).
- <sup>2</sup>F. M. Levinton, M. C. Zarnstorff, S. H. Batha, *et al.*, *Phys. Rev. Lett.* **75**, 4417 (1995).
- <sup>3</sup>E. J. Strait, L. L. Lao, M. E. Mauel, *et al.*, *Phys. Rev. Lett.* **75**, 4421 (1995).
- <sup>4</sup>T. Fujita, S. Idei, H. Shirai *et al.*, *Phys. Rev. Lett.* **78**, 2377 (1997).
- <sup>5</sup>O. Gruber, R. C. Wolf, R. Dux, *et al.*, *Phys. Rev. Lett.*, **83**, 1787 (1999).
- <sup>6</sup>Y. Koide, M. Kikuchi, M. Mori, *et al.*, *Phys. Rev. Lett.* **72**, 3662 (1994).
- <sup>7</sup>S. I. Lashkul, V. N. Budnikov, A.A. Borevich, *et al.*, *Plasma Phys. Control. Fusion* **42**, A169 (2000).
- <sup>8</sup>A. Fujisawa, H. Iguchi, T. Minami *et al.*, *Phys. Rev. Lett.* **82**, 2669 (1999).
- <sup>9</sup>P. Gohil, J. Kinsey, V. Parail, *et al.*, *Nucl. Fusion* **43**, 707 (2003).
- <sup>10</sup>J. E. Rice, R. L. Boivin, P. T. Bonoli, *et al.*, *Nucl. Fusion* **41**, 277 (2001).
- <sup>11</sup>C. L. Fiore, J. E. Rice, P. T. Bonoli, *et al.*, *Phys Plasmas* **8**, 2023 (2001).
- <sup>12</sup>S. J. Wukitch, R. L. Boivin, P. T. Bonoli, *et al.*, *Phys. Plasmas* **9**, 2149 (2002).
- <sup>13</sup>J.E. Rice, P. T. Bonoli, E. S. Marmor, *et al.*, *Nucl. Fusion* **42**, 510 (2002).
- <sup>14</sup>E. J. Doyle, G. M. Staebler, L. Zeng, T.L. Rhodes, K. H. Burrell, C. M. Greenfield, R. J. Groebner, G. R. McKee, W. A. Peebles, C. L. Rettig, B. W. Rice, and B. W. Stallard, *Plasma Phys. Controlled Fusion* **42**, A237 (2000).
- <sup>15</sup>J. E. Rice, P. T. Bonoli, C. L. Fiore, *et al.*, *Nucl. Fusion* **43**, 781 (2003).
- <sup>16</sup>I. H. Hutchinson, R. Boivin, F. Bombarda, *et al.*, *Phys Plasmas* **1**, 1511 (1994).

- <sup>17</sup>Hawryluk, R., in Physics of Plasma Close to Thermonuclear Conditions, (Varenna,1979), Commission of the European Communities, Brussels, Vol. I, p. 61 (1979).
- <sup>18</sup>M. Brambilla, Plasma Physics and Controlled Fusion **41**, 1 (1999) .
- <sup>19</sup>M. Kotschenreuther, G. Rewoldt, and W. M. Tang, Comput. Phys Commun. **88**, 128 (1995).
- <sup>20</sup>M. H.Redl, D. R. Mikkelsen, G. Rewoldt, C. L. Fiore, P. T. Bonoli, D. R. Ernst, J. E. Rice, S. J. Wukitch, and W. Dorland, “Stability of Microturbulent Drift Modes During Internal Transport Barrier Formation in the Alcator C-Mod Radio Frequency Heated H-Mode”, submitted to Phys. Plasmas.
- <sup>21</sup>G. Tresset, X. Litaudon, D. Moreau, X. Garbet and Contributors to the EFDA-JET Work Programme, Nucl. Fusion **42**, 520 (2002).
- <sup>22</sup>D. R. Ernst, *et al.*, “Role of Trapped Electron Mode Turbulence in Internal Transport Barrier Control in Alcator C-Mod”, submitted to Phys. Plasmas.
- <sup>23</sup> V. Pericoli Ridolfini, E. Barbato, P. Buratti, *et al.*, Nuc. Fusion **6**, 469 (2003).
- <sup>24</sup>E. Joffrin, C.D. Challis, G. D. Conway, *et al.* Nucl. Fusion **43**, 1167 (2003).

## VII. Figure Captions

Fig 1. The profiles of the square root of the visible bremsstrahlung emission (a.) are shown as the ITB develops beginning with the H-mode and proceeding to a fully developed ITB for an off-axis ICRF heated discharge. The density peaking factor as a function of time is included for comparison (b). Electron density from Thomson scattering (c) is shown also.

Fig 2. The profiles of the square root of the visible bremsstrahlung emission (a) are shown as the ITB develops beginning with the H-mode and proceeding to a fully developed ITB for an Ohmic EDA plasma. The density peaking factor as a function of time (b) is included for comparison.

Fig. 3. The  $\chi_{\text{eff}}$  is seen to reach neoclassical levels at  $r/a \sim 0.3$  for both ITBs established in EDA Ohmic H-mode (a) and in off-axis ICRF cases (b).

Fig 4. The bootstrap current in the core increases 6-10 times as the ITB develops for both off-axis ICRF heated ITBs and EDA Ohmic H-mode ITBs.

Fig. 5. A calculation of the power density distribution in the off-axis ICRF ITB is compared to the power density distribution in an Ohmic EDA H-mode ITB during the initial ITB period and later after central ICRF has been added to both plasmas.

Fig. 6. Sawtooth oscillations in the electron temperature in the core of the plasma are shown for two discharges which were set up with the same target plasma and ICRF power, but with a.) 70 MHz frequency, off-axis deposition, with ITB and b.) 80 MHz, central deposition, no ITB.

Fig. 7. The electron temperature profiles are compared for the two discharges in Fig. 5 just before and after a sawtooth crash at  $t=1$  s when an ITB is developing in a.) the off-axis heated case and absent in b.) during on axis heating.



Fig.8. Dimensionless parameters  $\rho^*_T$ ,  $\rho^*_n$ , and  $\rho^*_p$  are shown as a function of radius during the ITB phase of the plasma created by using off-axis ICRF heating. The location of the barrier found from the density gradient is compared to the location of  $\eta_e=1$  and  $\rho^*_p > 0.014$ .

Fig. 9. The ITB foot location derived from the point  $\rho^*_p$  where exceeds 0.014 as a function of toroidal magnetic field (a) and (b) the ratio of plasma current to toroidal magnetic field are shown.

Fig. 10. The effect of incrementally adding central ICRF power to an Ohmically established ITB is shown on a.) the profiles and b.) the maximum density that is reached.

Fig. 11. The loss of peaking and the ITB when additional central ICRF power exceeds 0.6 MW is shown.

Fig. 12.  $\rho^*_p$  exhibits adverse effects from sawtooth oscillations when excessive central ICRF is added.

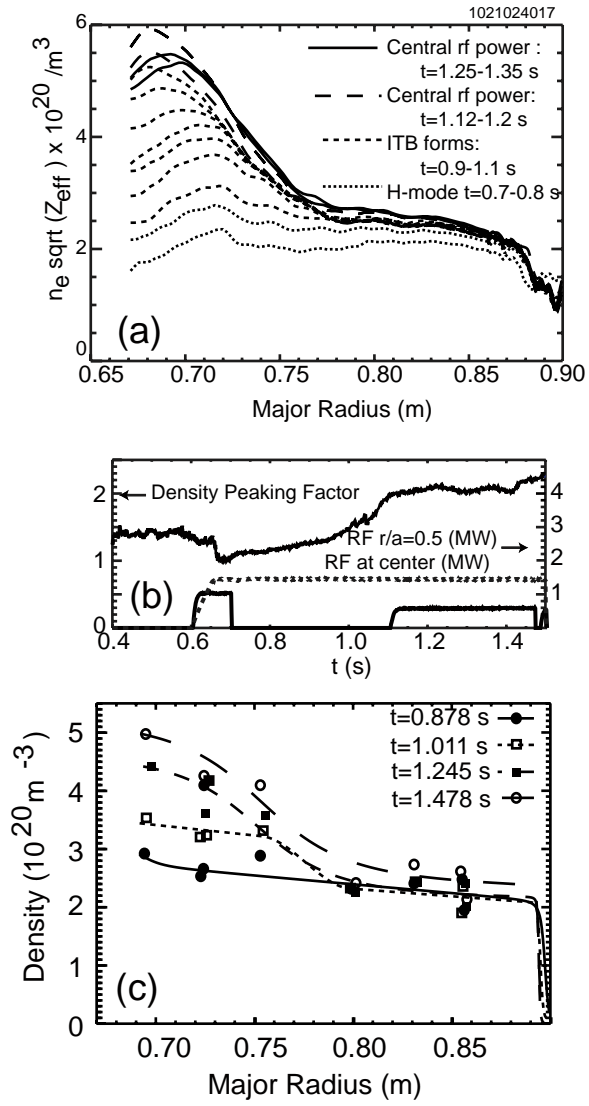


Figure 1.

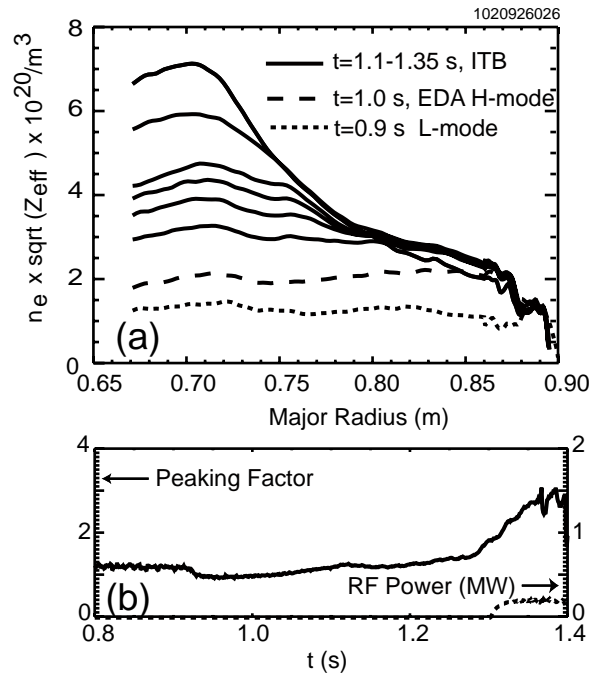


Figure 2.

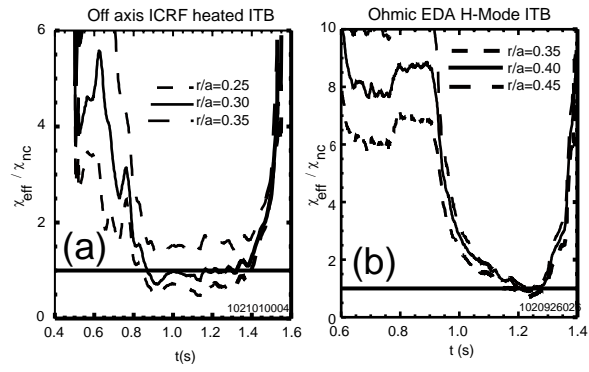


Figure 3.

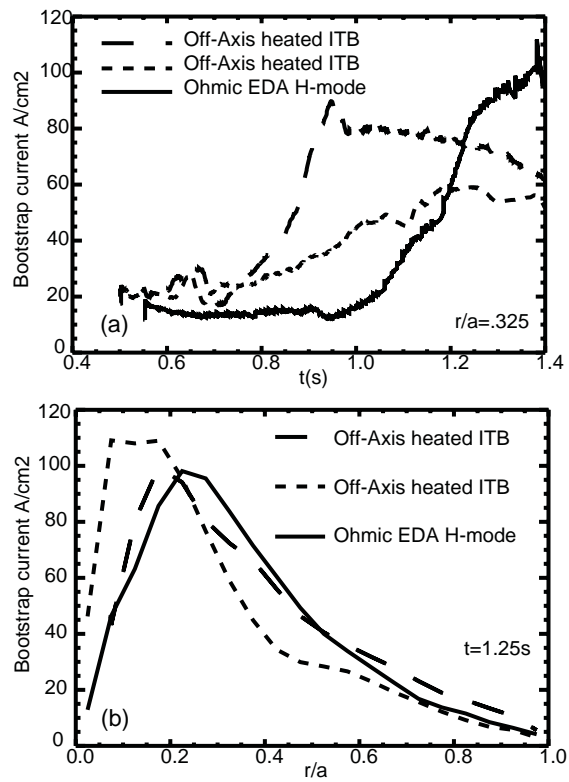


Figure 4.

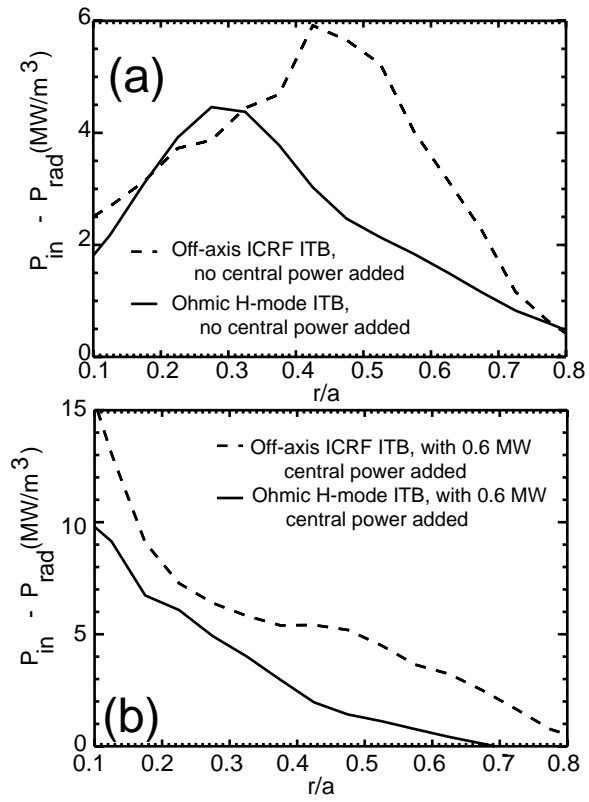


Figure 5

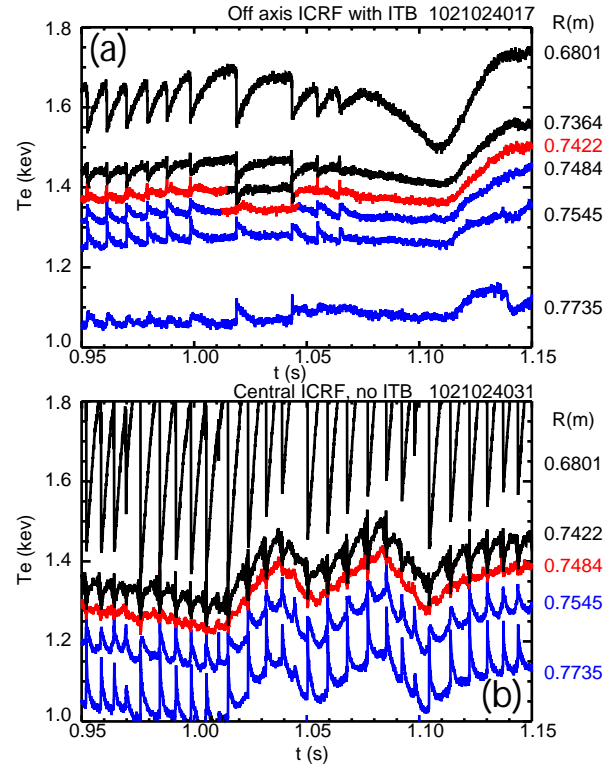


Figure 6

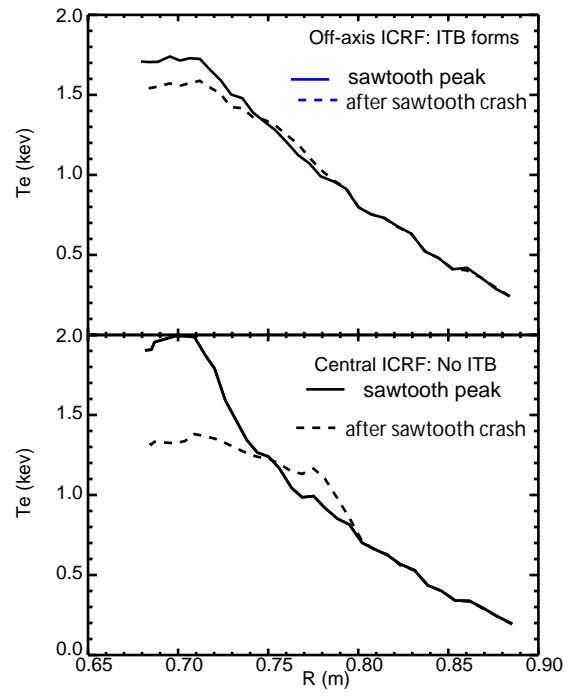


Figure 7



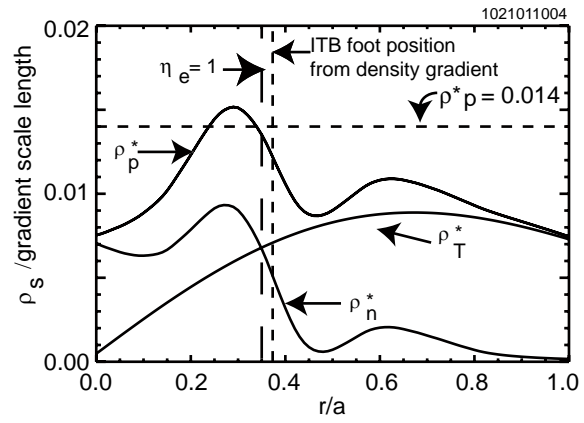
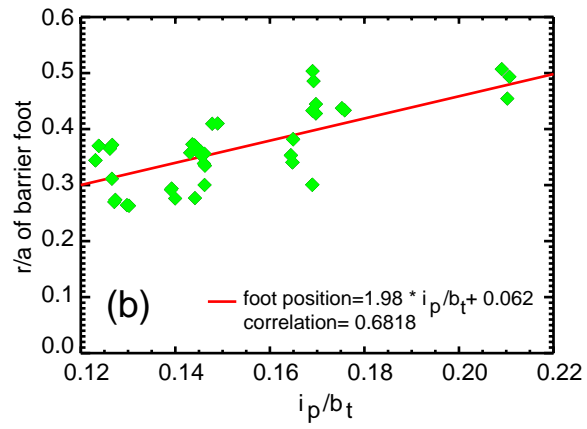
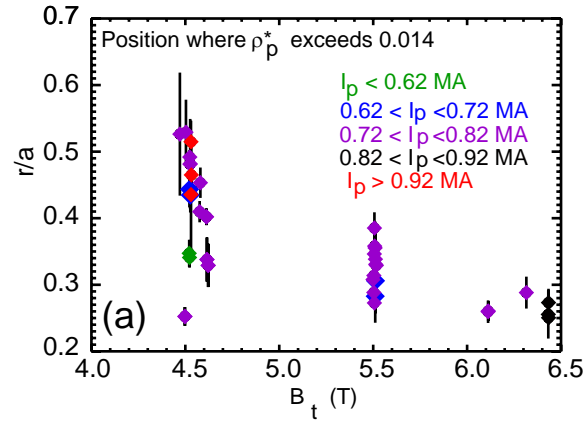


Figure 8



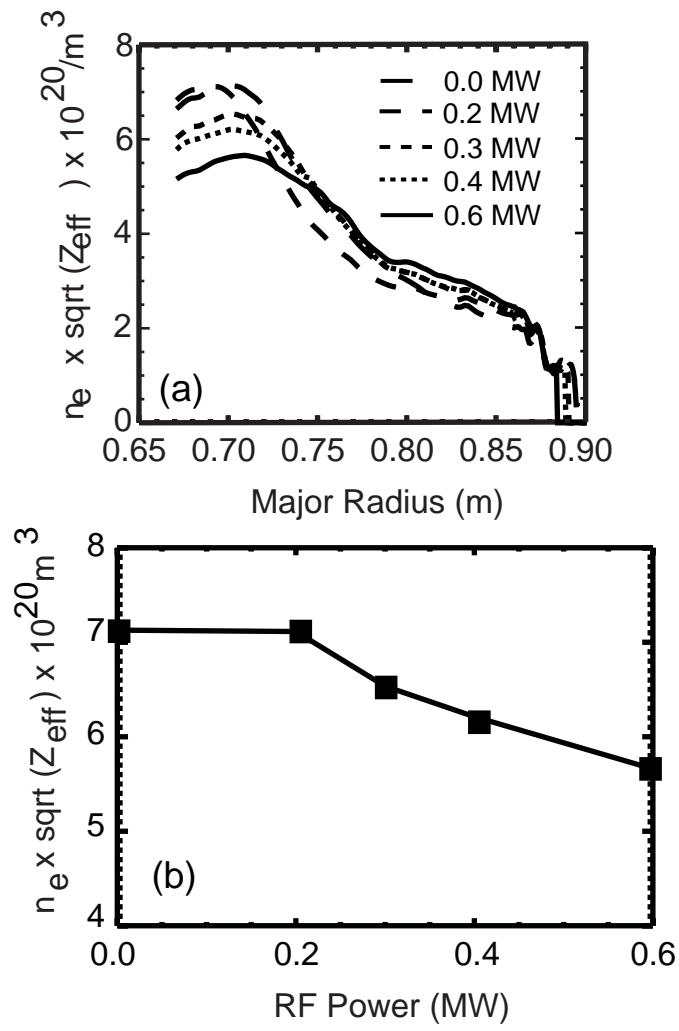


Figure 10

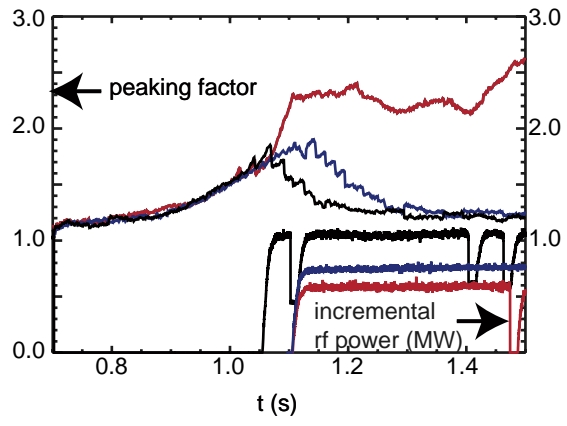


Figure 11

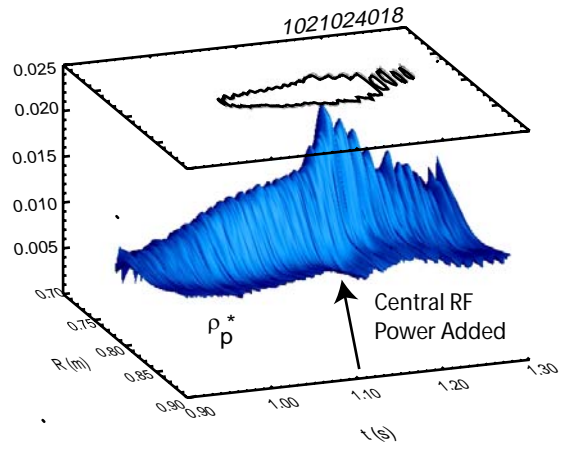


Figure 12